*35th EPS Conference on Plasma Phys. Hersonissos, 9 - 13 June 2008 ECA Vol.**32D**, P-1.105 (2008)*

# Systematic study of impurity pellet injection with Z=6-74 for improvement of plasma performance in LHD

S.Morita[1], R.Sakamoto[1], M.B.Chowdhuri[2], M.Goto[1], K.Ida[1], K.Ikeda[1], O.Kaneko[1], K.Nagaoka[1], K.Narihara[1], Y.Oka[1], M.Osakabe[1], S.Sakakibara[1], Y.Takeiri[1], K.Tanaka[1], K.Tsumori[1], K.Y.Watanabe[1], I.Yamada[1], M.Yokoyama[1], M.Yoshinuma[1], H.Y.Zhou[2]

[1]*National Institute for Fusion Science, Toki 509-5292, Gifu, Japan*

[2]*Dept. of Fusion Science, Graduate Univ. for Advanced Studies, Toki 509-5292, Gifu, Japan*

In helical plasmas experiments on pellet injection have been extensively done in relation to the study of high-density operation with improvement of plasma performance because the current-driven instability can be basically ruled out. Impurity pellets with atomic number of Z=6 to 74 have been injected in NBI $H_2$ plasmas of Large Helical Device (LHD) and the plasma response has been studied in low and high density regions. In case of the carbon pellet, the plasma performance is scaled by 1.5 times to the ISS95-scaling, which is close to the $H_2$ pellet injection case, and the high $T_i(0)$ up to 5keV has been achieved with peaked density profiles in low-density operation (~$1.5\times10^{13}$cm$^{-3}$).

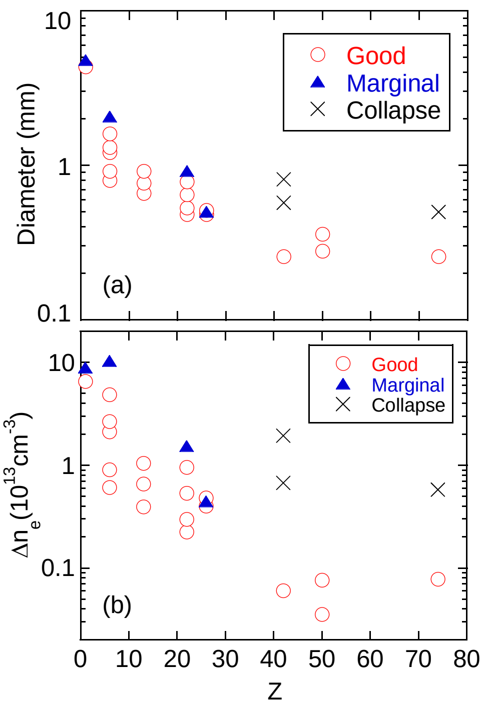


Fig.1 Plasma response after pellet injection (H,C, Al, Ti, Fe, Mo, Sn and W); Z dependence for (a) diameter and (b) density rise.

The size and speed of injected pellets range in 0.3-1.8mm depending on Z and 100-300m/s depending on weight and size, respectively [1]. Heavier pellets generally have lower speed. The plasma response after the pellet injection has been investigated in relation to the size and density rise systematically changing the Z number (H, C, Al, Ti, Fe, Mo, Sn and W). The results are shown in Fig.1 (a) and (b). Maximum size of the pellets, $S_{max}$, which can maintain a discharge without plasma collapse under $P_{in}$~10-18MW, is $3.4^{\phi}$mm×$3.4$mm$^{L}$ in cylinder for an $H_2$ ice pellet and $1.8^{\phi}$mm×$1.8$mm$^{L}$ for a carbon pellet. The 3.8mm $H_2$ and 2.0mm carbon pellets were tried, but the smooth operation of discharges was a little difficult. The $S_{max}$ of course decreases with Z, i.e., ~1mm for Al and Ti and 0.2-0.3mm for Mo and W. The density rise, $\Delta n_e$, is close to $10\mathrm{x}10^{14}\mathrm{cm}^{-3}$ for single $H_2$ and carbon pellet injection. However, the upper limit of $\Delta n_e$ reduces down to $1\mathrm{x}10^{13}\mathrm{cm}^{-3}$ for Al pellet. The access to high-density operation is therefore limited to both of $H_2$ and C pellets.

The impurity pellet can control its deposition in plasma radius by adjusting heating scenario and a kind of pellets, although the control is difficult for single $H_2$ pellet injection. This is due to a large difference in the sublimation energy, i.e., 0.005eV for $H_2$ and a few eV for C. Typical examples for C pellet injection are shown in Figs.2 (a) and (b). In Fig.2 (a) the C pellet is deposited at ρ=0.8 and in Fig.2 (b) the pellet is evaporated at plasma center. In order to deposit the pellet into deep inside of the plasma core the effect of fast ions has to be taken into account [2]. The ratio of $T_e$ to neutral beam energy is generally large in helical devices. Since the negative-ion-based high-energy NBI with $E_{NBI}$=180keV is mainly used in LHD, the ratio becomes also large even in high-temperature discharges with $T_e$=2-4keV. The beam slowing down time, $\tau_s$, becomes longer, e.g., $\tau_s$=1s at $n_e \sim 0.5\mathrm{x}10^{13}\mathrm{cm}^{-3}$. The $\tau_s$ is approximately equal to $\tau_E$ at $\sim 3\mathrm{x}10^{13}\mathrm{cm}^{-3}$ and the stored fast ion energy, $W_{NBI}$, is bigger than $W_p$ in such a low-density range. As a result, the heat flux, Q (≡nvT), coming into the pellet through the fast ions, becomes huge compared with the thermal heat flux, e.g., $Q_{fast}/Q_{thermal} \sim 30$ at $n_e = 1\mathrm{x}10^{13}\mathrm{cm}^{-3}$. In Fig.2 (b), therefore, the C pellet is injected at the same time as the start time of the 2nd NBI heating to avoid the outer evaporation due to the fast ions.

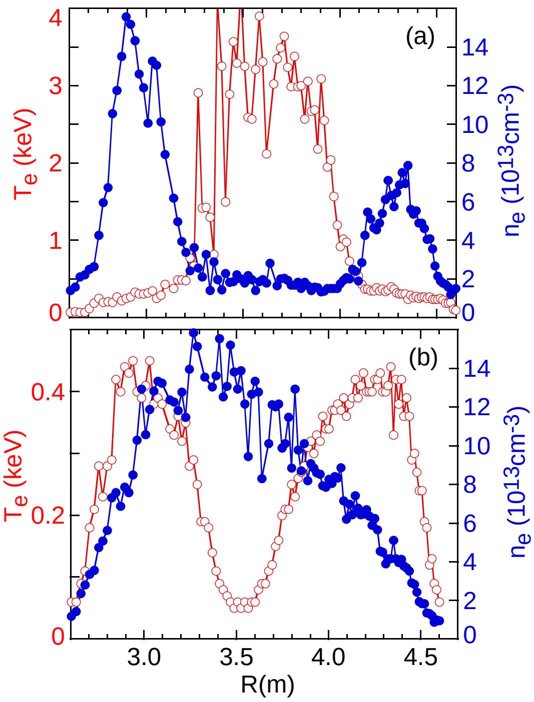

Fig.2 $T_e$ and $n_e$ profiles for different C pellet deposition; (a) ρ=0.8, (b) ρ=0.0. Calibration is now in progress for the tentative $n_e$ profiles.

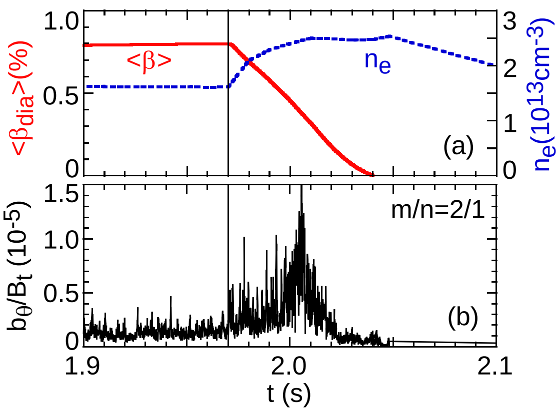

Fig.3 MHD behavior at plasma collapse induced by Mo pellet injection; (a) β-value decay, (b) m/n=2/1 amplitude.

When the C pellet is deposited at the plasma center, an extremely hollow $T_e$ profile appears as shown in Fig.2 (b), whereas the peaked $n_e$ profile is formed. The hollow $T_e$ profile is kept during 50ms after the pellet injection and begins to recover the peaked $T_e$ profile. Here, remarkably important thing should be mentioned that the discharge is quite stable even in such a hollow pressure profile case. In relation to this, MHD stability has been examined in NBI discharges with plasma collapse after pellet injection. The spherical Mo pellet with a diameter of 0.5mm is used for the purpose. A typical result is shown in Figs.3 (a) and (b). After the injection the beta value measured from diamagnetic loop decreases monotonically whereas the density gradually goes up and keeps a constant density increment until the complete disappearance of the plasma energy. The decay time of the plasma energy is approximately equal to $\tau_E$ of the discharge. In such collapsed phases any strong MHD mode excitation has not been observed. In Fig.3 (b) the m/n=2/1 mode fluctuation is plotted, but the amplitude is quite small. It is thus concluded that the plasma collapse following after the impurity pellet injection is not induced by the MHD instability [3].

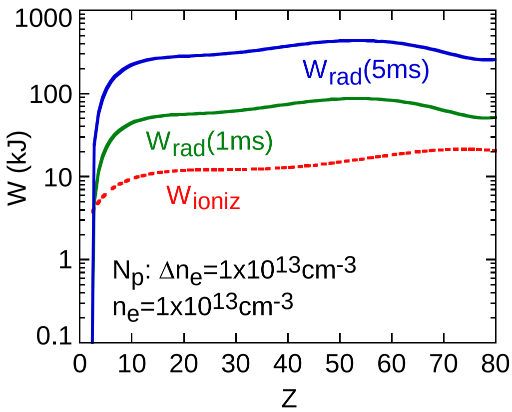


Fig.4 Radiation loss $W_{rad}$ during (a) 1ms and (b) 5ms after pellet injection and ionization loss $W_{ioniz}$.

The energy loss processes after the impurity pellet injection are basically thought to be ionization and radiation losses. The ionization loss is the total summation of ionization energies necessary for ionizing the impurity ions up to a charge state equivalent to $T_e$. The radiation loss is principally equal to the electron excitation loss which is determined by the total summation of collisional excitation in each change state of the impurity ions. The calculation is done as a function of Z under conditions of $n_e$=1x10$^{13}$cm$^{-3}$, $\Delta n_e$=1x10$^{13}$cm$^{-3}$ and $T_e$=2keV. The result is shown in Fig.4. The radiation loss energy, $W_{rad}$, is a function of ionization speed of the impurity ions, which largely depends on the temperature behavior of the background plasma after the pellet injection. The ionization time seems to be order of 1ms for carbon ($C^0$=>$C^{6+}$). However, the exact estimation of the ionization time is really difficult at least now because of the lack of plasma parameters in the ablation cloud. The $W_{rad}$ in Fig.4 does not include radiation loss from intrinsic background impurities which is enhanced by the reduction of temperature. It is clear that the $W_{rad}$ is much higher than the $W_{ioniz}$. The $W_{rad}$ is bigger than the energy stored within a certain flux tube determined by the pellet ablation size and is also bigger than the input power. This result suggests that the plasma collapse after the impurity pellet injection is induced by the breaking of the thermal balance.

The plasma performance after C pellet injection is compared with gas puffing and $H_2$ pellet injection as shown in Fig.5 ($R_{ax}$=3.60m). The $W_p$ is scaled by the Stellalator scaling of ISS95 to eliminate the difference in the NBI input power ($5 \le P_{NBI} \le 18$MW). In case of the pellet injection the maximum $W_p$ observed during the density decay phase are plotted. The data for the $H_2$ pellet are obtained from multi-pellets injection, whereas those for the C pellet are from single-pellet injection. The operational range is then different for each other (C: 2-4x$10^{13}$cm$^{-3}$, $H_2$: 4-10x$10^{13}$cm$^{-3}$). In LHD the confinement improvement has been observed so far compared to the ISS95-scaling, as indicated with "1.5×ISS95". The performance on the present C pellet injection also shows the similar confinement to the $H_2$ pellet.

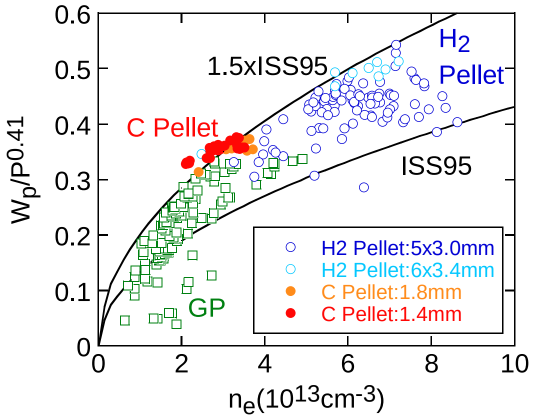


Fig.5 Performance of C pellet injection normalized by ISS95 input power scaling ($W_p$[MW], P [MW])

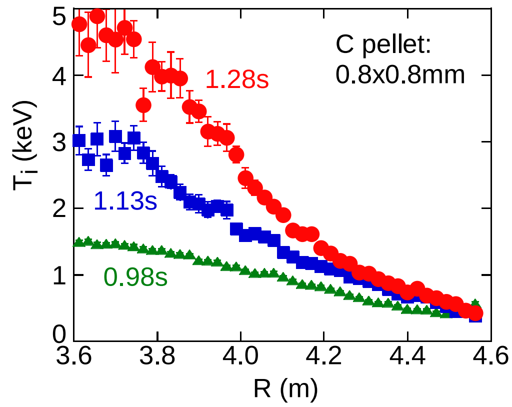


Fig.6 High $T_i$ operation with C pellet injected at t=0.95s.

A small C pellet (0.8-1.2mm) has been injected into low-density $H_2$ discharges ($1.0 \le n_e \le 1.5$x$10^{13}$cm$^{-3}$). A high-ion temperature is often observed at the density decay phase as shown in Fig.5 [4]. The C pellet is injected at t=0.9s. The centrally peaked ion temperature profile is formed after 0.3s with $T_i(0)$=5keV. The ablation of the C pellet in the present case is occurred at ρ=0.4. The central deposition of the pellet as seen in Fig.2 (b) does not increase the $T_i(0)$ so high. The maintenance of relatively high $T_e(0)$ is possibly the key for the formation of high-$T_i$ discharge in addition to the formation of the peaked density. Similar discharges with high $T_i(0)$ are also obtained in Al and Ti pellet injection.

References


[1] H.Nozato, S.Morita, M.Goto et al., Rev.Sci.Instrum. 74, 2032 (2003).

[2] S.Morita, Y.Shirai, M.Goto et al., Nucl.Fusion 42, 876 (2002).

[3] S.Morita, E.Kawatoh, K.Ohkubo et al., Nucl.Fusion 30, 938 (1990).

[4] S.Morita, H.Nozato et al., Journal of Plasma and Fusion Research 79, 641 (2003).